Chinese Journal of Natural Medicines

A polysaccharide from *Arthrospira platensis* alleviates pancreatic cancerassociated with negatively regulating galectin-3 and glypican-6 expression

Rakotomalala Manda Heriniaina, Xia Chen, Yulian Wu, Wenfeng Liao, He Fei, Peipei Wang, Kan Ding

Citation: Rakotomalala Manda Heriniaina, Xia Chen, Yulian Wu, Wenfeng Liao, He Fei, Peipei Wang, Kan Ding, A polysaccharide from *Arthrospira platensis* alleviates pancreatic cancerassociated with negatively regulating galectin-3 and glypican-6 expression, Chinese Journal of Natural Medicines, 2026, 24(2), 227-236. doi: 10.1016/S1875-5364(26)61093-X.

View online: https://doi.org/10.1016/S1875-5364(26)61093-X

Chinese Journal of Natural Medicines 24 (2026) 227-236

Contents lists available at ScienceDirect

Chinese Journal of Natural Medicines

journal homepage: www.cjnmcpu.com/

Original article

A polysaccharide from *Arthrospira platensis* alleviates pancreatic cancer associated with negatively regulating galectin-3 and glypican-6 expression

Rakotomalala Manda Heriniaina[a,Δ], Xia Chen[a,Δ], Yulian Wu[c, a], Wenfeng Liao[a], He Fei[a], Peipei Wang[a, b,*], Kan Ding[a, c,*]

[a] *Glycochemistry and Glycobiology Lab, Key Laboratory of Receptor Research, Shanghai Institute of Materia Medica, Chinese Academy of Sciences, University of Chinese Academy of Sciences, Shanghai 201203, China*

[b] *Key Laboratory for Chemistry and Molecular Engineering of Medicinal Resources, Guangxi Normal University, Guangxi 541004, China*

[c] *School of Chinese Materia Medica, Nanjing University of Chinese Medicine, Nanjing 210029, China*

ARTICLE INFO

Article history:
Received 26 January 2025
Revised 8 April 2025
Accepted 14 July 2025
Available online 20 February 2026

Keywords:
Pancreatic cancer
Galectin-3
Glypican-6
Polysaccharide
Arthrospira platensis

ABSTRACT

Pancreatic cancer, specifically pancreatic ductal adenocarcinoma (PDAC), ranks among the most prevalent malignancies and is a leading cause of cancer-related mortality worldwide. Therefore, there is an urgent need to identify novel anti-pancreatic cancer agents. This study reports a newly identified homogeneous polysaccharide, designated ESPPW, isolated from *Arthrospira platensis* (*A. platensis*). The molecular weight of ESPPW is estimated at 356 kDa, and it consists predominantly of glucose and rhamnose, with minor amounts of mannose, glucuronic acid, galacturonic acid, galactose, xylose, arabinose, and fucose. ESPPW inhibits the proliferation and migration of PDAC cells both *in vitro* and *in vivo*. Mechanistic investigations reveal that ESPPW induces apoptosis through activation of caspase-3 and is associated with upregulation of the tumor-suppressor protein p53. Notably, treatment with 2.8 nmol·L^{-1} of ESPPW leads to significant time-dependent downregulation of galectin-3 (Gal-3) and glypican-6 (GPC-6). These findings are corroborated by immunohistochemical analysis of tumor xenograft tissues. Furthermore, overexpression of Gal-3 and GPC-6 reverses the pro-apoptotic effect of ESPPW, as indicated by restored cycle regulatory proteins (CDK2) expression. In conclusion, these data demonstrate that ESPPW suppresses PDAC cell growth by promoting apoptosis and disrupting the functional activity of Gal-3 and GPC-6.

1. Introduction

Pancreatic cancer, characterized as either adenocarcinoma (≥ 95% of cases) or endocrine tumors (≤ 5% of cases) [1], is among the leading causes of cancer morbidity and mortality worldwide. By 2030, pancreatic ductal adenocarcinoma (PDAC) is projected to become the second leading cause of cancer-related deaths in the United States and Europe based on current incidence rates [2]. The 5-year survival rate for patients diagnosed with PDAC remains only about 4% [3]. Currently, surgical resection represents the primary treatment option; however, only approximately 25% of patients are eligible at diagnosis. Most patients present at advanced stages—locally advanced (30%) or metastatic (> 50%). Furthermore, tumor recurrence occurs in 60% to 80% of patients within three years after curative-intent surgery [4].

Despite ongoing progress in cancer research, the lack of effective and specific therapeutic targets continues to hinder advancements in pancreatic cancer treatment. Glypicans (GPCs), comprising six members (GPC-1 to GPC-6), are a subgroup of heparan sulfate proteoglycans (HSPGs) that are tethered to the cell surface *via* glycosylphosphatidylinositol (GPI) anchors and also reside within the extracellular matrix. Structurally, GPCs consist of a core protein of approximately 60–70 kDa with one or more covalently attached glycosaminoglycan chains [5]. Multiple studies have demonstrated that HSPGs are overexpressed in various cancers and play critical roles in growth factor signaling pathways [5-7], as well as in cell-cell interactions, migration, and cell-matrix adhesion [6]. The involvement of GPCs in tumorigenesis has been extensively studied. Gao et al. reported that GPCs regulate cell proliferation and function as essential co-receptors for fibroblast growth factors (FGFs) and Wnts [8, 9]. Downregulation of GPC-1 significantly reduces levels of certain FGFs, including FGF-2, HB-EGF, and TGF-β1 [10, 11]. Silencing GPC-1 also induces apoptosis in esophageal cancer cells by inhibiting epidermal growth factor receptor (EGFR), Akt, and p44/42-mitogen-activated protein kinase (MAPK) signaling pathways [12]. Similarly, GPC-2 is highly expressed in neuroblastoma and contributes to tumor progression by activating the Wnt/*β*-catenin signaling pathway [13]. GPC-3 is associated with suppression of metastasis and can activate non-canonical Wnt/c-Jun *N*-terminal kinase (JNK) and p38 signaling in breast cancer [14]. GPC-4 activates the *β*-catenin pathway by

* Corresponding author.
E-mail addresses: ppwang@shou.edu.cn (P. Wang); dingkan@simm.ac.cn (K. Ding)
Δ These authors contributed equally to this work.

https://doi.org/10.1016/S1875-5364(26)61093-X

binding with Wnt3a and Wnt5a [15]. Additionally, GPC-5 may promote rhabdomyosarcoma proliferation *via* hedgehog signaling activation [16]. In contrast, the role of the GPC-6 in cancer remains comparatively underexplored. Recent evidence indicates that knockdown of GPC-6 reduces tumor cell proliferation and colony formation while increasing expression of pro-apoptotic caspase-3 [17, 18]. GPC-6 has also been shown to interact with Wnt5a [18] and promote breast cancer progression by activating the Wnt5a/JNK/p38 MAPK signaling cascade, which is linked to metastatic phenotypes [19].

Galectin-3 (Gal-3), a unique chimera-type member of the 16-member *β*-galactoside-binding Gal family, features a carbohydrate recognition domain connected to an unusually long *N*-terminal proline- and glycine-rich domain [20]. Notably, Gal-3 overexpression correlates with high tumor grade and lymph node metastasis [21]. Tsutomu et al. demonstrated that Gal-3-mediated invasion involves regulation of GSK-3β phosphorylation and *β*-catenin degradation in pancreatic cancer cells [22]. More recently, Gal-3 has been implicated in signaling pathways associated with pancreatic cancer development [23, 24].

Arthrospira platensis (*A. platensis*), a blue-green photoautotrophic microalga, was first identified in the Kanem region of Chad. It has been used as a nutritional supplement since ancient times due to its high protein content and medicinal properties [25, 26]. Numerous studies have documented beneficial bioactive effects of *A. platensis*, including anti-tumor and anti-oxidant activities [27, 28]. Konícková et al. reported that extracts of *A. platensis* exhibit anti-proliferative activity against pancreatic cancer cells [29]. In this study, we investigated the anti-pancreatic cancer activity and underlying mechanisms of polysaccharides derived from *A. platensis*.

2. Materials and methods

2.1. Materials and chemicals

The powder of *A. platensis* was purchased from Yunnan Here Biotechnology Co., Ltd. (Yunnan, China). Dialysis bags (MWCO = 3500 Da) were obtained from Shanghai Green Bird Company (Shanghai, China). Food-grade cellulase (U = 2000) was acquired from Shandong Lonza Enzymes Co., Ltd. (Shandong, China), while food-grade papain (U = 400 000) and amylase (U = 1 000 000) were sourced from Nanning Pangbo Biological Engineering Co., Ltd. (Guangxi, China). DEAE Sepharose Fast Flow was provided by GE Healthcare. Standard monosaccharides—galactose (Gal, lot#: c10087798), glucose (Glc, lot#: c14286805), mannose (Man, lot#: c10082642), rhamnose (Rha, lot#: c10044523), glucuronic acid (GlcA, lot#: c17290227), galacturonic acid (GalA, lot#: c14286790), xylose (Xyl, lot#: c10027023), arabinose (Ara, lot#: c100699973), and fucose (Fuc, lot#: c14254981)—were purchased from Shanghai Aladdin Bio-Chem Technology Co., Ltd. (Shanghai, China). Trifluoroacetic acid (TFA) was obtained from Sinopharm Chemical Reagent Co., Ltd. (Shanghai, China). 3-(4,5-Dimethylthiazol-2-yl)-2,5-diphenyl tetrazolium bromide (MTT) and Giemsa were acquired from Sigma-Aldrich, USA; Trizol reagent was from Invitrogen. Dimethyl sulfoxide (DMSO) was supplied by E. Merck (Germany). Dulbecco's modified Eagle medium (DMEM, glutamine, high glucose), RPMI-1640 medium, penicillin, streptomycin, and fetal bovine serum (FBS) were purchased from Gibco, Thermo Fisher Scientific (USA). Other reagents were of analytical grade and obtained from Sinopharm Chemical Reagent Co., Ltd. (Shanghai, China).

2.2. Extraction and purification of polysaccharides from *A. platensis*

Dried *A. platensis* powder (180 g) was soaked in ethanol (95%, 5 L) for two weeks. After ethanol removal, the residue was extracted with water at 55 °C (10 L) using enzymatic assistance (0.03 mol·L^{-1} cellulase, 0.005 mol·L^{-1} papain, and 0.01 mol·L^{-1} amylase) under stirring for 1 h. Enzymes were inactivated by heating the solution to 100 °C. The extract was filtered to remove insoluble material and concentrated to approximately 2 L. This concentrate was dialyzed against flowing water for 48 h using a dialysis membrane with a molecular weight cutoff of 3500 Da. The retentate was concentrated to about 2 L and centrifuged, and the supernatant was precipitated with five volumes of 95% ethanol overnight. The resulting precipitate was collected by centrifugation (14 430 × *g*, 10 min), dissolved in 1 L of deionized water, and freeze-dried to yield crude polysaccharide ESPP (16 g, 8.9% yield). ESPP (5 g) was dissolved in distilled water (50 mL) and centrifuged (14 430 × *g*, 10 min). The supernatant was subjected to anion-exchange chromatography on a DEAE Sepharose™ Fast Flow column eluted with deionized water and 0.1, 0.2, and 0.4 mol·L^{-1} NaCl. Four fractions were collected: ESPPW (254 mg, 0.14%), ESPP0.1 (108 mg, 0.06%), ESPP0.2 (286 mg, 0.16%), and ESPP0.4 (187 mg, 0.10%). The designation "ESPP" refers to enzyme-extracted polysaccharides from *A. platensis*, with suffixes indicating elution solvent concentration. Among the fractions, only ESPPW was confirmed as a homogeneous polysaccharide, while the remaining fractions required further purification. A schematic representation of the extraction and purification procedure is illustrated in Fig. 1.

2.3. Physical and chemical properties of ESPPW

The homogeneity, molecular weight, total carbohydrate content, protein content, and monosaccharide composition of ESPPW were evaluated using previously reported methods [30]. Briefly, 2 mg of ESPPW was hydrolyzed with 2 mol·L^{-1} TFA at 121 °C, followed by derivatization with 1-phenyl-3-methyl-5-pyrazolone (PMP). Monosaccharide composition was analyzed by HPLC [31] using a Fortis C_{18} column (5 μm, 4.6 mm × 250 mm) on an Agilent 1200 system equipped with a G1362A Binpump and G1314F UV detector.

2.4. Cell cultures

All cell lines were obtained from the Type Culture Collection Center of the Chinese Academy of Sciences (Shanghai, China). Hu-

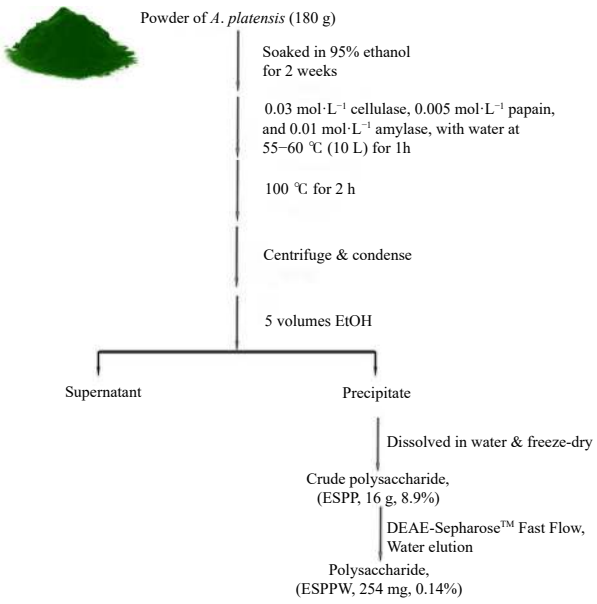

Fig. 1 The procedures of ESPPW extraction and purification.

man PDAC cell lines AsPC-1 and BxPC-3, along with the normal pancreatic epithelial cell line human pancreatic cell line (HPDE6-C7), were cultured in DMEM (Gibco, Thermo Fisher Scientific, USA) supplemented with 10% FBS and 1% penicillin/streptomycin. Cells were maintained in a humidified incubator at 37 °C with 5% CO_2.

2.5. MTT proliferation assay and colony formation assays

To assess the inhibitory effects of polysaccharide fractions on pancreatic cancer cell viability (AsPC-1 and BxPC-3), MTT assays were performed. Cells were seeded at 3×10^3 cells per well in 96-well plates and treated with ESPPW at concentrations of 0.35, 0.70, 1.4, and 2.8 nmol·L^{-1} for 72 h. MTT solution (5 mg·mL^{-1}, Sigma-Aldrich, USA) was added to each well, and cells were incubated at 37 °C for 4 h. Absorbance at 490 nm was measured using a microplate reader (Novostar, Becton Dickinson, USA). Viability was expressed as a percentage relative to untreated controls, arbitrarily set at 100%. For colony formation assays, AsPC-1 and BxPC-3 cells (1000 cells/well) were seeded in 35 mm dishes and treated with ESPPW at 0, 1.4, and 2.8 nmol·L^{-1}. The medium was replaced every three days. After two weeks, colonies were stained with Giemsa and counted.

2.6. Migration assays

Cell migration of BxPC-3 and AsPC-1 (2×10^5 cells) was evaluated using wound-healing assays. Cells were seeded in 6-well plates and serum-starved for 24 h. A scratch wound was created manually, and cells were washed and incubated with fresh medium containing 1% FBS and ESPPW at 1.4 or 2.8 nmol·L^{-1}. Images were captured at 0 and 24 h to monitor wound closure. Migrated cells were visualized using a light microscope (Olympus BX51).

2.7. Ribonucleic acid (RNA) extraction, reverse transcription-polymerase chain reaction (RT-PCR), and quantitative real-time PCR

Total RNA was extracted from cells cultured in complete medium for 48 h using Trizol reagent (Invitrogen, USA) according to the manufacturer's instructions. Briefly, cells were washed with phosphate-buffered saline (PBS), lysed with Trizol, mixed thoroughly, and chloroform was added. After vigorous shaking and centrifugation, the aqueous phase containing RNA was collected. Total RNA was reverse-transcribed into cDNA using murine leukemia virus reverse transcriptase [M-MLV, Taq kit (TaKaRa); Otsu, Shiga, Japan]. Semi-quantitative RT-PCR was performed to assess mRNA expression of *GPC-6* and *Gal-3*. Primers were synthesized by Sangon Biotech (Shanghai, China): *GPC-6* forward: 5'-CAG GGA TGT GGT CAG CCC AA-3', reverse: 5'-CTT GTG CCT GCA GCA GTT GT-3'; *Gal-3* forward: 5'-CCA AAG AGG GAA TGA TGT TGC C-3', reverse: 5'-TGA TTG TAC TGC AAC AAG TGA GC-3'; glyceraldehyde-3-phosphate dehydrogenase (*GAPDH*) forward: 5'-GTA ATT GGC GCC TGG TCA CC-3', reverse: 5'-CAG TGG ACT CCA CGA CGT AC -3'. Amplification conditions included initial denaturation at 95 °C for 34 s, annealing at 60 °C (*GPC-6*), 54 °C (*Gal-3*), or 58 °C (*GAPDH*) for 30 s, and extension at 72 °C for 30 s. Quantitative real-time PCR was conducted using an Applied Biosystems 7900 Fast Real-Time PCR System with SYBR Green Premix Ex Taq (TaKaRa, Japan). Each sample was run in triplicate, and C_t values (threshold cycle) were recorded. *GAPDH* served as the internal control for normalization.

2.8. Western blotting analysis

To evaluate the anti-pancreatic cancer effects of ESPPW and determine whether it modulates Gal-3 and GPC-6 expression, Western blotting was performed. BxPC-3 and AsPC-1 cells were lysed in the presence of a 1% proteinase inhibitor cocktail under varying treatment conditions. Protein samples (about 36 μg) were separated by SDS-PAGE and transferred to PVDF membranes (BioRad). Membranes were blocked with TBST buffer [20 mmol·L^{-1} Tris (pH 8.0), 150 mmol·L^{-1} NaCl, 0.1% Tween-20] containing 5% non-fat milk for 2 h, then incubated overnight at 4 °C with primary antibodies diluted 1∶1000 used: Gal-3 (Santa Cruz Biotechnology Shanghai Co., Ltd., Shanghai, China), GPC-6, cleaved caspase-3, cyclin A2, CDK2, and p53 (Cell Signaling Technology), and GAPDH (Abmart). After washing, membranes were incubated with HRP-conjugated secondary anti-rabbit or anti-mouse antibodies (Abmart) for 2 h. Signal detection was performed using an enhanced chemiluminescence (ECL) substrate.

2.9. Detection of caspase-3 activity

Caspase-3 activity was measured using a colorimetric assay kit (Beyotime, Haimen, China) following the manufacturer's protocol [32].

2.10. Cell cycle analysis

Cells (3×10^5 cells/well) were seeded in 6-well plates and allowed to adhere overnight. After 48 h of ESPPW treatment, cells were harvested with 0.25% trypsin, washed with cold PBS, and fixed in ice-cold 75% ethanol at 4 °C overnight. Following washing, cells were incubated with RNase A (100 μg·mL^{-1}) at 37 °C for 30 min, then stained with propidium iodide (PI, 50 μg·mL^{-1}, Invitrogen) on ice for 15 min. Deoxyribonucleic acid (DNA) content was analyzed by flow cytometry using CellQuest Pro software (BD Bioscience, USA). Cell cycle distribution was determined using ModFit cell analysis software.

2.11. Hoechst 33258 staining

Hoechst 33258 staining was performed using a kit from Wanleibio Co., Ltd. (Shenyang, China). Logarithmically growing cells were seeded into 12-well plates (2×10^6 cells/well) with coverslips and cultured at 37 °C for 24 h. Cells were fixed with 4% paraformaldehyde for 20 min at room temperature, stained with 2 μL·mL^{-1} Hoechst solution, and rinsed twice with phosphate-buffered saline. Coverslips were mounted, and nuclear morphology was examined under a fluorescence microscope (IX53; Olympus Corporation, Tokyo, Japan) to detect apoptotic nuclei.

2.12. Xenograft model and immunohistochemistry

Female athymic nude (nu/nu) mice (5 weeks old, 18–20 g) were obtained from the Shanghai Laboratory Animal Center, Chinese Academy of Sciences. All procedures were approved by the Institutional Animal Care and Use Committee (IACUC) of the Shanghai Institute of Materia Medica (May 15, 2019) and conducted in accordance with institutional guidelines. BxPC-3 cells (5×10^6) were injected subcutaneously into the left flank to establish tumors. Forty mice were divided into four groups (n = 10): control, gemcitabine-treated (positive control), low-dose ESPPW, and high-dose ESPPW. Treatment began when tumors became palpable (15 days post-injection). ESPPW was administered *via* tail vein injection at 5 or 50 mg·kg^{-1} every 48 h for 15 days; gemcitabine (40 mg·kg^{-1}) and normal saline (control) were given similarly. Tumor size and body weight were monitored weekly. On day 30, mice were euthanized, and tumors were excised, fixed in 4% paraformaldehyde, paraffin-embedded, and sectioned for immunohistochemical analysis. Primary antibodies against Gal-3 (1∶100, Santa Cruz Biotechnology, USA), GPC-6 (1∶500, Cell Signaling Technology, USA), and KRAS (1∶200, ABclonal, Inc., China) were used. Semi-quantitative image analysis was performed us-

ing Image Pro Plus software.

2.13. Lentiviral transduction for gene overexpression and knockdown

Lentiviral vectors for *GPC-6* overexpression and knockdown were constructed using pLVX-IRES-ZsGreen (OBiO Technology Corp., Ltd., China). For *Gal-3*, the vector pLenti-EF1a-mCherry-P2A-Puro-CVM-MCS-3Flag was used (OBiO Technology Corp., Ltd., China). Viral particles were produced by co-transfecting HEK293T cells with packaging plasmids (2 mol·L^{-1} $CaCl_2$, PMD2.G, PSPAX2) and 2 × HBS solution per well, as described previously [24].

2.14. Statistical analysis

Each experiment was independently repeated at least three times. Data were analyzed using one-way ANOVA and unpaired, two-tailed Student's *t*-tests. Graphs and curves were generated using GraphPad Software, Inc. (CA, USA).

3. Results

3.1. The properties of ESPPW

Crude polysaccharide (ESPP) was extracted from *A. platensis* powder using enzyme-assisted hot water extraction. A homogeneous fraction, ESPPW, was purified from ESPP *via* DEAE Sepharose™ Fast Flow column chromatography using water as the eluent. ESPPW had a molecular weight of 356 kDa (Fig. 2), contained 99.8% ± 1.6% carbohydrate, and trace protein (0.2% ± 2.0%). Its monosaccharide composition was predominantly glucose and rhamnose (Table 1).

Table 1 The monosaccharide composition of ESPPW.

Monosaccharide	Man	Rha	GlcA	GalA	Glc	Gal	Xyl	Ara	Fuc
Ratio (%)	5.8	30.6	4.5	4.0	39.1	5.0	2.5	2.4	6.2

3.2. ESPPW inhibited the growth of pancreatic cancer cells in vitro and in vivo

Among all four fractions, ESPPW exhibited the highest inhibitory activity against AsPC-1 and BxPC-3 cells. Subsequent studies focused on ESPPW to evaluate its effects on a normal human pancreatic duct epithelial cell line (HPDE6-C7) and to determine whether tumor cell inhibition resulted from polysaccharide-induced cytotoxicity. ESPPW was applied at concentrations ranging from 0.35 to 2.8 nmol·L^{-1} to AsPC-1, BxPC-3, and HPDE6-C7 cells for 72 h. As shown in Fig. 3A, ESPPW significantly suppressed the proliferation of AsPC-1 and BxPC-3 cells in a concentration-dependent manner. In contrast, ESPPW treatment did not impair the viability of HPDE6-C7 cells. Furthermore, based on half maximal inhibitory concentration (IC_{50}) values of 0.27 nmol·L^{-1}, BxPC-3 cells were identified as the most sensitive pancreatic cancer cell line to ESPPW. Consistently, colony formation assays demonstrated that clonogenic capacity was markedly reduced even at a concentration of 1.4 nmol·L^{-1} in both AsPC-1 and BxPC-3 cells (Fig. 3B).

To extend these observations, we evaluated the anti-tumor effects of ESPPW in nude mice bearing BxPC-3 xenografts. After 15 days of intravenous administration of ESPPW (5–50 mg·kg^{-1}, once every 2 days), tumor growth in treated animals was significantly slower than in the control group. Similarly, tumor weight was reduced upon completion of treatment (Figs. 4A–4C). Notably, the anti-tumor efficacy of ESPPW was comparable to that of gemcitabine. Additionally, ESPPW treatment did not cause significant changes in mouse body weight during the study period (Fig. 4D).

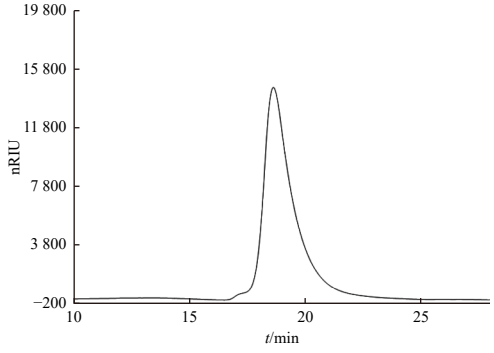

Fig. 2 The HPGPC spectrum of ESPPW.

3.3. ESPPW restrained cell migration, activated apoptosis, and induced pancreatic cancer cell cycle arrest

ESPPW markedly inhibited the migration of BxPC-3 and AsPC-1 cells at concentrations of 1.4 and 2.8 nmol·L^{-1} (Figs. 5A and 5B). Investigation into apoptosis induction revealed that ESPPW increased caspase-3 activity (Fig. 5C) and significantly upregulated the expression of pro-apoptotic cleaved caspase-3 (Figs. 5D and 5E) and the tumor suppressor p53 (Figs. 5F and 5G). To further explore the mechanism underlying ESPPW-mediated growth inhibition, flow cytometric analysis was performed on BxPC-3 and AsPC-1 cells treated with 2.8 nmol·L^{-1} ESPPW after PI staining. A higher proportion of cells accumulated in the S phase, indicating S-phase cell cycle arrest (Figs. 6A and 6B). This arrest is critical, as it may trigger apoptotic pathways when DNA damage or replication stress prevents cell cycle progression. As shown in Fig. 6C, Hoechst 33258 staining revealed increased dense particle fluorescence, nuclear shrinkage, and chromatin condensation in ESPPW-treated cells, further confirming the induction of apoptosis. Additionally, ESPPW treatment led to a concentration-dependent decrease in the expression of both cyclin A2 and CDK2 (Figs. 6D and 6E), key regulators of cell cycle progression. Downregulation of these proteins correlates with impaired cell cycle progression and can promote apoptosis. These findings suggest that ESPPW induces apoptosis in pancreatic cancer cells through S-phase arrest and subsequent activation of apoptotic signaling.

3.4. ESPPW inhibited Gal-3 and GPC-6 expression

As previously reported, Gal-3 plays a role in suppressing apoptosis and promoting cell survival in pancreatic cancer cells [33]. Upon exposure of BxPC-3 and AsPC-1 cells to 2.8 nmol·L^{-1} ESPPW for varying durations (12–72 h), the expression levels of Gal-3 and GPC-6 were significantly downregulated in a time-dependent manner relative to controls (Figs. 7A–7D). Immunohistochemical analysis further confirmed that ESPPW treatment strongly suppressed Gal-3 and GPC-6 expression in tumor tissues (Fig. 7E). Notably, overexpression of either Gal-3 or GPC-6 attenuated the inhibitory effects of ESPPW on cyclin A2 and CDK2 expression (Supporting Figs. 1A, 1B, and Figs. 7F, 7G). As expected, ESPPW treatment (2.8 nmol·L^{-1}) for 72 h induced caspase-3 cleavage in pancreatic cancer cells overexpressing GPC-6 and Gal-3 (Figs. 8A and 8B). Furthermore, ESPPW treatment significantly reduced colony size in BxPC-3 and AsPC-1 cells overexpressing GPC-6 or

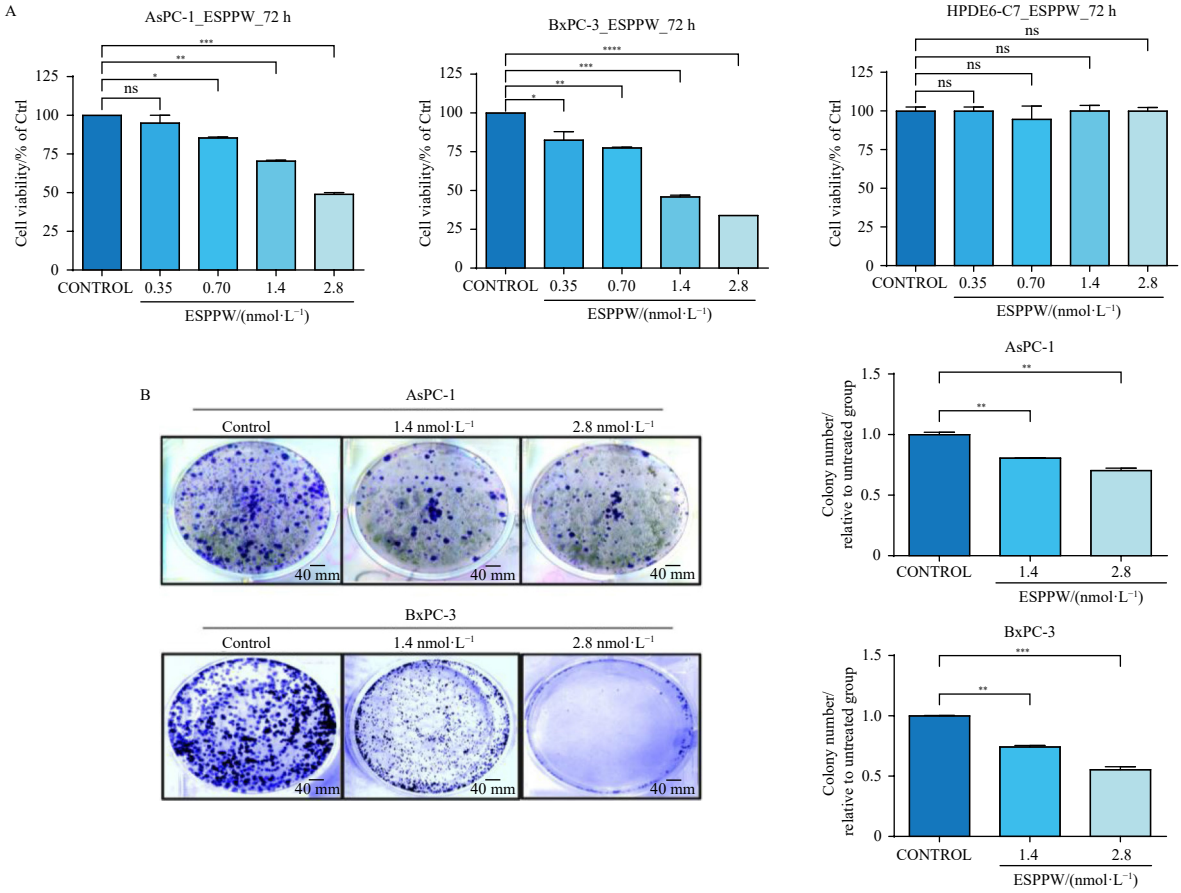

Fig. 3 ESPPW inhibited pancreatic cancer cell viability and colony formation. (A) Cell viability of AsPC-1, BxPC-3, and normal pancreatic epithelial cells HPDE6-C7 were evaluated using the MTT assay after 72 h of incubation with ESPPW at various concentrations (0, 0.35, 0.70, 1.4, 2.8 nmol·L^{-1}). (B) Representative images of colony formation assays in AsPC-1 and BxPC-3 cells following ESPPW treatment (1.4 and 2.8 nmol·L^{-1}) for 2 weeks, with colony numbers quantified for statistical analysis (right panel), scale bar: 10 mm. Data are presented as mean ± SD. All experiments were performed in triplicate. Statistical significance was determined using a two-tailed Student's *t*-test. $^{*}P < 0.05$, $^{**}P < 0.01$, $^{***}P < 0.001$, $^{****}P < 0.0001$.

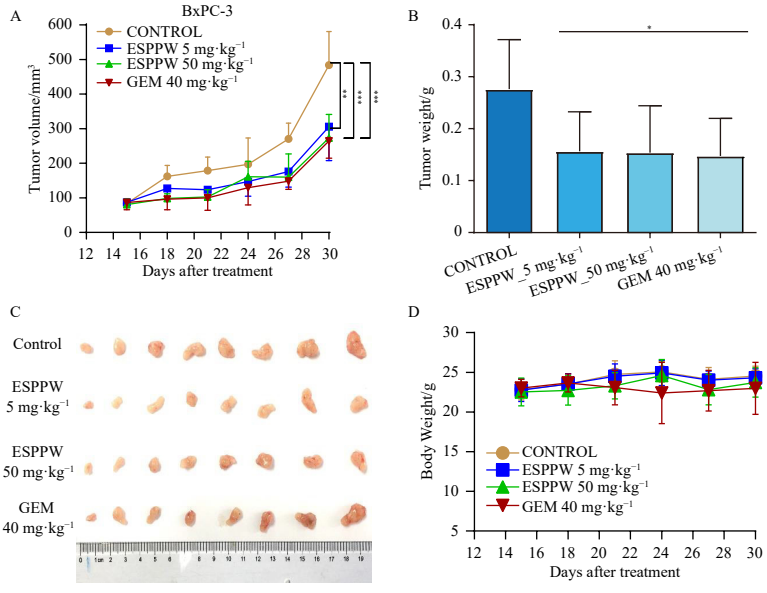

Fig. 4 ESPPW inhibited the growth of tumor xenografts in mice. (A) Tumor growth curves showed the average tumor volumes in mice treated with ESPPW for two weeks, compared to those untreated or treated with gemcitabine (GEM, 40 mg·kg^{-1}). (B) Final tumor weights measured at the end of the treatment period. (C) Representative images of excised tumors from each treatment group. (D) Body weight monitoring throughout the experiment. Data are presented as mean ± SD. All experiments were performed in triplicate. Statistical analysis was performed using a two-tailed Student's *t*-test. $^{*}P < 0.05$, $^{**}P < 0.01$, $^{***}P < 0.001$, $^{****}P < 0.0001$.

Gal-3 compared to untreated controls (Figs. 8C and 8D). Additionally, knockdown of GPC-6 and Gal-3 led to decreased expression of CDK2 and cyclin A2, along with increased levels of pro-apoptotic p53 and cleaved caspase-3 (Supporting Figs. 2 and 3).

4. Discussion

Water-soluble polysaccharides from *A. platensis* have been widely reported to exhibit diverse bioactive properties, including

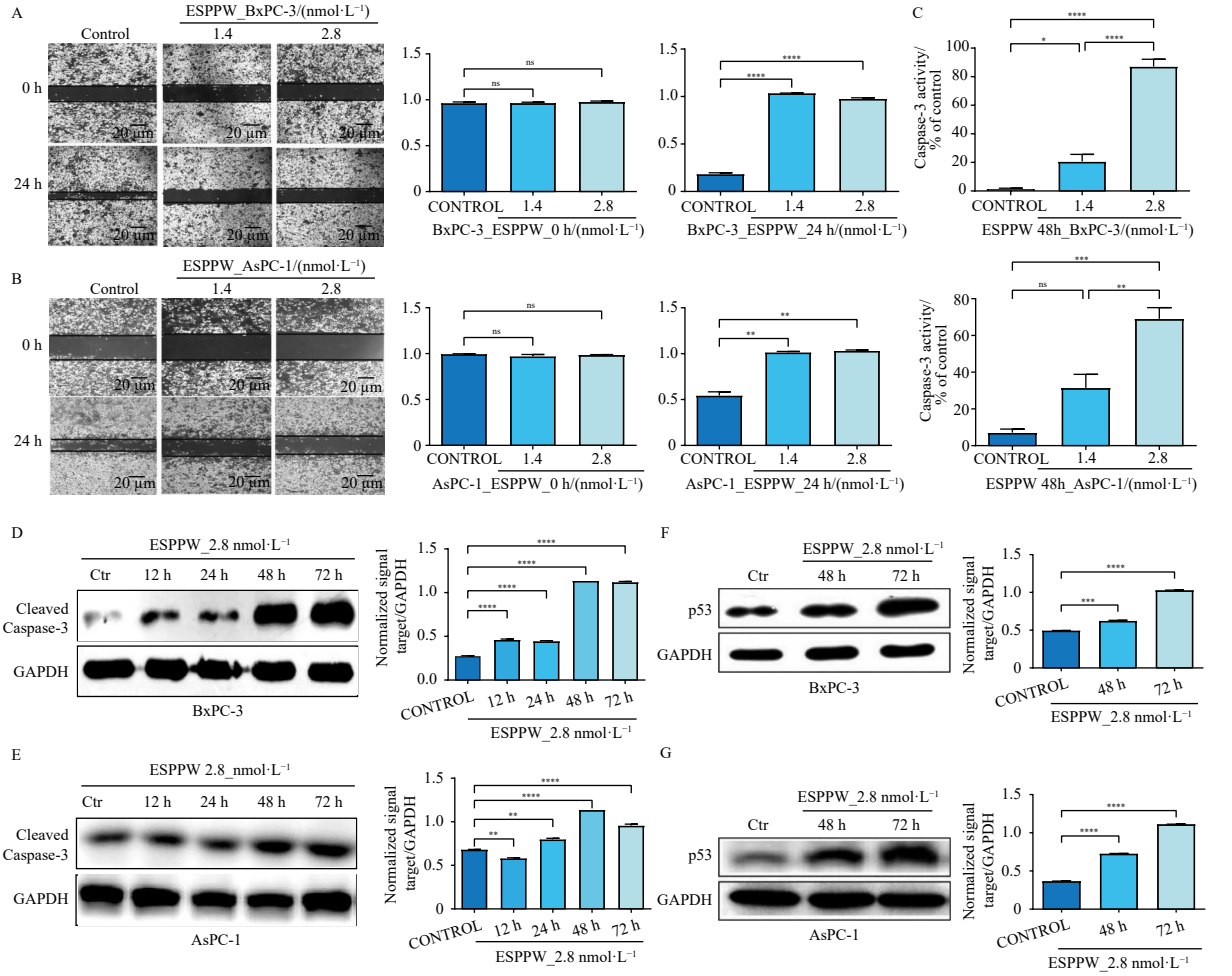

Fig. 5 ESPPW inhibited the migration and induced apoptosis of BxPC-3 cells *in vitro*. (A and B) Wound-healing assays demonstrated that ESPPW treatment (1.4 and 2.8 nmol·L^{-1}) for 24 h significantly inhibited the migratory capacity of BxPC-3 and AsPC-1 pancreatic cancer cells. Images were captured at a 40 × magnification, scale bar: 20 μm. (C) Caspase-3/7 activity assays showed increased caspase activation in BxPC-3 and AsPC-1 cells treated with ESPPW (1.4 and 2.8 nmol·L^{-1}) for 48 h compared to untreated controls. (D and E) Western blotting analysis confirmed elevated levels of cleaved caspase-3 in response to ESPPW treatment. (F, G) Expression of p53 was also upregulated following ESPPW exposure. Data are presented as mean ± SD. All experiments were performed in triplicate. Statistical significance was determined using a two-tailed Student's *t*-test. $^{*}P < 0.05$, $^{**}P < 0.01$, $^{***}P < 0.001$, $^{****}P < 0.0001$.

pro-apoptotic, anti-oxidant, and anti-proliferative effects across various cancer cell lines [29, 34, 35]. Chu et al. demonstrated that *A. platensis* extract exhibits greater protective activity against free radical-induced apoptotic cell death than vitamin C or vitamin E [36]. A recent study indicated that a water extract from *A. platensis* inhibits the growth of PA-TU-8902 pancreatic cancer cells by enhancing VEGF and other angiogenic factor production [37]; however, the precise composition of the extract remains undefined. To date, no studies have linked the anti-cancer effects of *A. platensis* polysaccharides to the regulation of Gal-3 or GPC-6 expression. In this study, we investigated the anti-pancreatic cancer activity and underlying mechanisms of ESPPW, a water-soluble polysaccharide with an average molecular weight of 35.6 × 10^4 Da isolated from *A. platensis* powder. First, we validated previous findings and hypotheses regarding the potent anti-tumor activity and low toxicity of *A. platensis* extracts. MTT assays revealed that ESPPW induced dose- and time-dependent growth inhibition in two human pancreatic cancer cell lines (AsPC-1 and BxPC-3), with an average IC_{50} value of 0.27 nmol·L^{-1}. ESPPW also effectively suppressed tumor growth in BxPC-3 xenograft-bearing mice. Consistent with prior research, overexpression of the tumor suppressor p53 promotes apoptotic cell death [38]. Our results demonstrate that ESPPW significantly induces tumor cell apoptosis by upregulating p53 and cleaved caspase-3. Gal-3, a member of the *β*-galactoside-binding lectin family, exerts anti-apoptotic functions during tumorigenesis [39]. Wild-type p53 downregulates Gal-3, and this suppression is essential for p53-mediated apoptosis [40]. Our study shows that ESPPW downregulates Gal-3 expression in pancreatic cancer cells, which correlates with reduced levels of cell cycle regulators (CDK2 and cyclin A2) and elevated pro-apoptotic proteins (cleaved caspase-3 and p53). These effects were corroborated by shRNA-mediated *Gal-3* knockdown. These data suggest that ESPPW may induce apoptosis *via* Gal-3-mediated modulation of cell cycle and apoptotic pathways. More recently, Filmus et al. reported that GPC-6 knockout in intestinal epithelial cells enhances cleaved caspase-3 expression and triggers apoptosis through Wnt5a signaling, as GPC-6 interacts with Wnt5a to inhibit its pro-apoptotic activity [18, 41]. ESPPW-mediated GPC-6 downregulation may disrupt the Wnt5a/JNK/p38 MAPK signaling axis, a key pathway regulating proliferation [42], apoptosis [43], and cell cycle progression [44] in cancer. As a well-established activator of non-canonical Wnt signaling, Wnt5a maintains cellular homeostasis by activating JNK and p38 MAPK [44]. Therefore, disruption of GPC-6, which potentially modulates Wnt5a activity, may reduce JNK and p38 MAPK activation, thereby decreasing cell survival and promoting apoptosis in pancreatic cancer cells. Additionally, our findings indicate that GPC-6 knockdown reduces CDK2 and cyclin A2 expression while increasing cleaved caspase-3 and p53 levels. Based on existing literature, we hypothesize potential cooperation between Gal-3 and GPC-6, as both are implicated in EGFR/ERK downstream signaling pathways [24, 45]. Notably, NG2, a transmembrane chondroitin

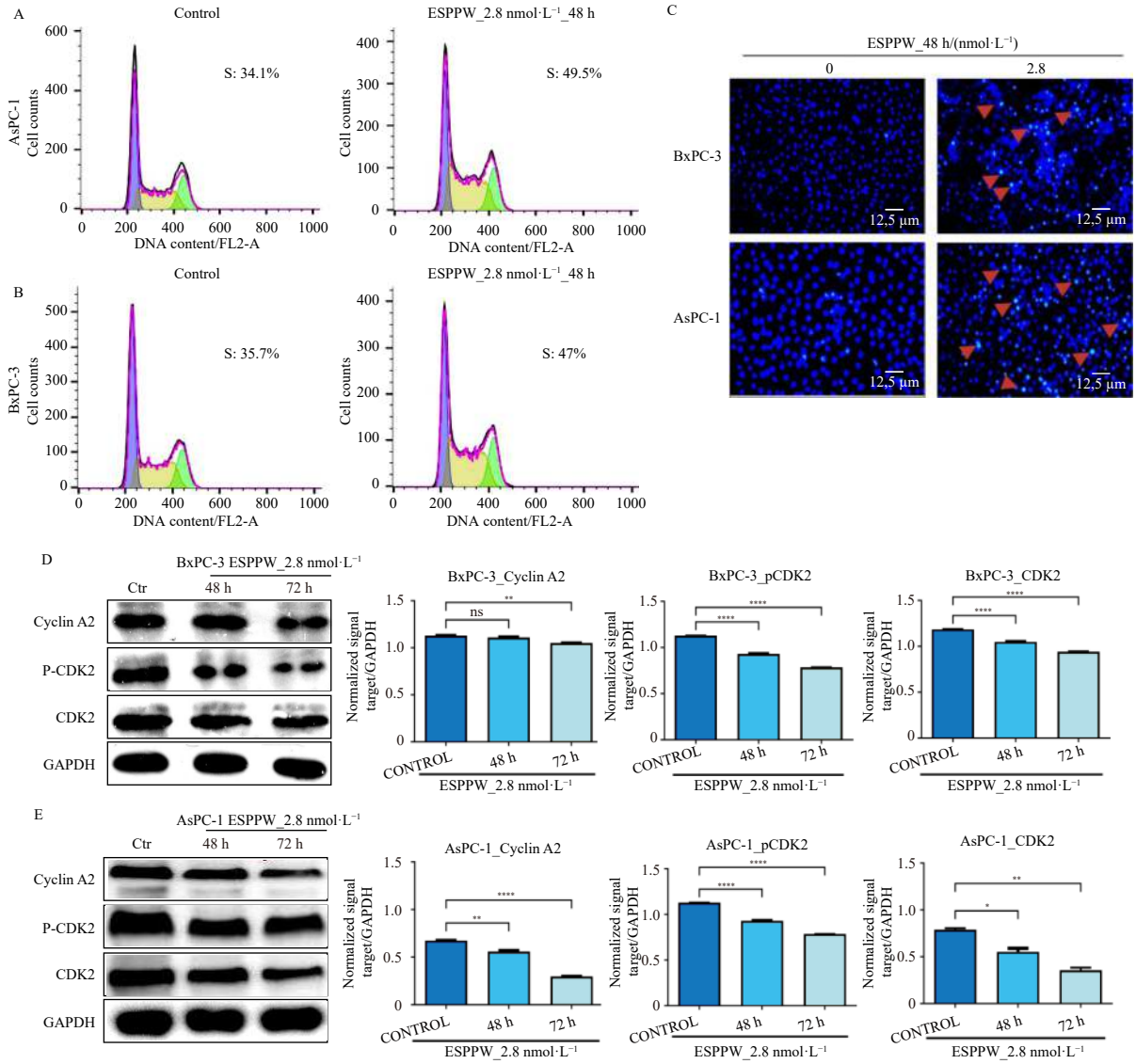

Fig. 6 ESSPW inhibited cell cycle progression and induced apoptosis in pancreatic cancer cells. (A and B)) Flow cytometry analysis of cell cycle distribution in BxPC-3 and AsPC-1 cells after 48 h of treatment with 2.8 nmol·L^{-1} ESPPW. (C) Hoechst 33258 staining revealed distinct nuclear morphology changes in BxPC-3 and AsPC-1 cells following 2.8 nmol·L^{-1} ESPPW treatment. Scale bar: 12.5 μm. (D and E) Western blotting analysis of cell cycle regulatory proteins, including cyclin-A2, p-CDK2, and CDK2 in BxPC-3 and AsPC-1 cells treated with ESPPW. Data are presented as mean ± SD. All experiments were conducted in triplicate. Statistical significance was determined using a two-tailed Student's *t*-test. $^{*}P < 0.05$, $^{**}P < 0.01$, $^{***}P < 0.001$, $^{****}P < 0.0001$.

sulfate proteoglycan, has been shown to interact with both Gal-3 and α3β1 integrin, stimulating integrin-mediated signaling and activating FAK and ERK pathways [46, 47].

Our data confirm that ESPPW treatment downregulates Gal-3 and GPC-6 protein expression *in vitro* (in AsPC-1 and BxPC-3 cells) and *in vivo* (in xenograft models), as determined by West-

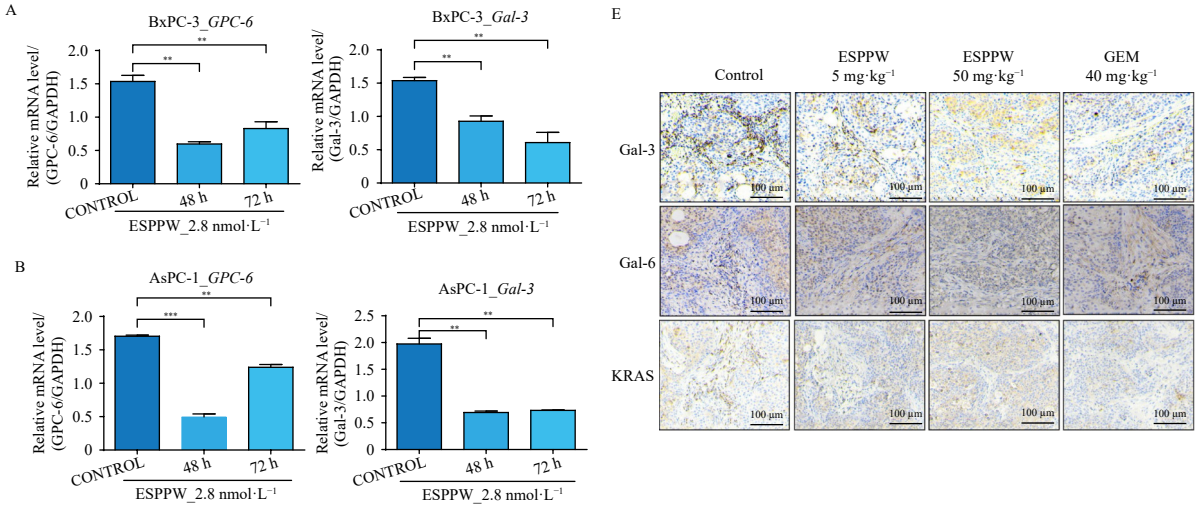

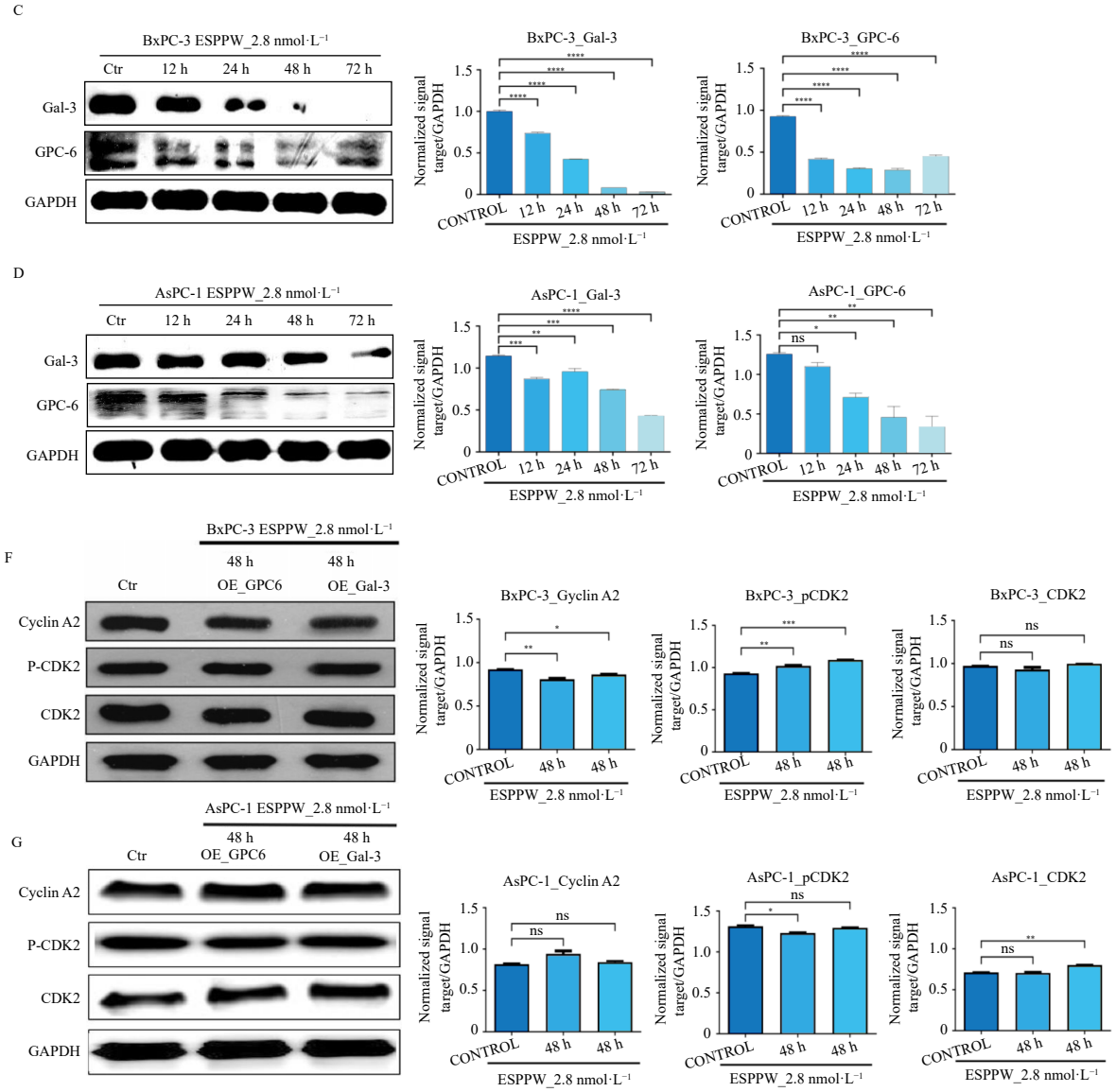

Fig. 7 ESPPW inhibited Gal-3 and GPC-6 expression in pancreatic cancer cells, inducing apoptosis, wherea overexpression of these proteins reversed these effects. (A and B) mRNA expression levels of *Gal-3* and *GPC-6* in BxPC-3 and AsPC-1 cells were analyzed by RT-qPCR analysis after treatment with 2.8 nmol·L^{-1} ESPPW. (C and D) Protein expression levels of Gal-3 and GPC-6 were examined by Western blotting in BxPC-3 and AsPC-1 cells following treatment with 2.8 nmol·L^{-1} ESPPW. (E) Immunohistochemical analysis of Gal-3 and GPC-6 expression in xenograft tumor tissues derived from BxPC-3 cells (from Fig. 4C), comparing vehicle- and ESPPW-treated group (Scale bar: 100 μm). (F and G) Effects of ESPPW on apoptotic proteins Cyclin-A2, p-CDK2, and CDK2 were detected by Western blotting assay in BxPC-3 and AsPC-1 cells transfected with Gal-3 and GPC-6 overexpression constructs. Data are presented as mean ± SD. All experiments were performed in triplicate. Statistical significance was evaluated using a two-tailed Student's *t*-test. $^{*}P < 0.05$, $^{**}P < 0.01$, $^{***}P < 0.001$, $^{****}P < 0.0001$.

ern blotting and immunohistochemical analyses. Previous studies from our group demonstrated that polysaccharides RN1 and HH1-1 from *Panax notoginseng* effectively reduce Gal-3 expression and bind to EGFR, thereby disrupting the Gal-3–EGFR interaction and inhibiting PDAC cell growth *in vitro*, *in vivo*, and in patient-derived xenografts. These compounds also affect cancer cell proliferation, cell cycle, apoptosis, angiogenesis, migration, and invasion. Whether ESPPW similarly interferes with Gal-3 binding to receptors such as EGFR, thereby blocking Gal-3-mediated protumorigenic signaling, warrants further investigation [23, 24]. Moreover, ESPPW-induced downregulation of cyclin A2 and CDK2 represents a crucial mechanism contributing to apoptosis in certain pancreatic cancer cells. Importantly, overexpression of either Gal-3 or GPC-6 counteracts the pro-apoptotic effects of ESPPW, including CDK2 suppression and caspase-3 activation. This indicates that ESPPW-mediated downregulation of Gal-3 and

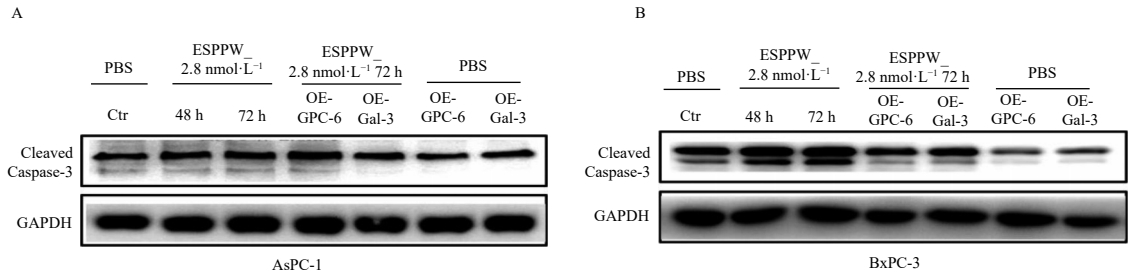

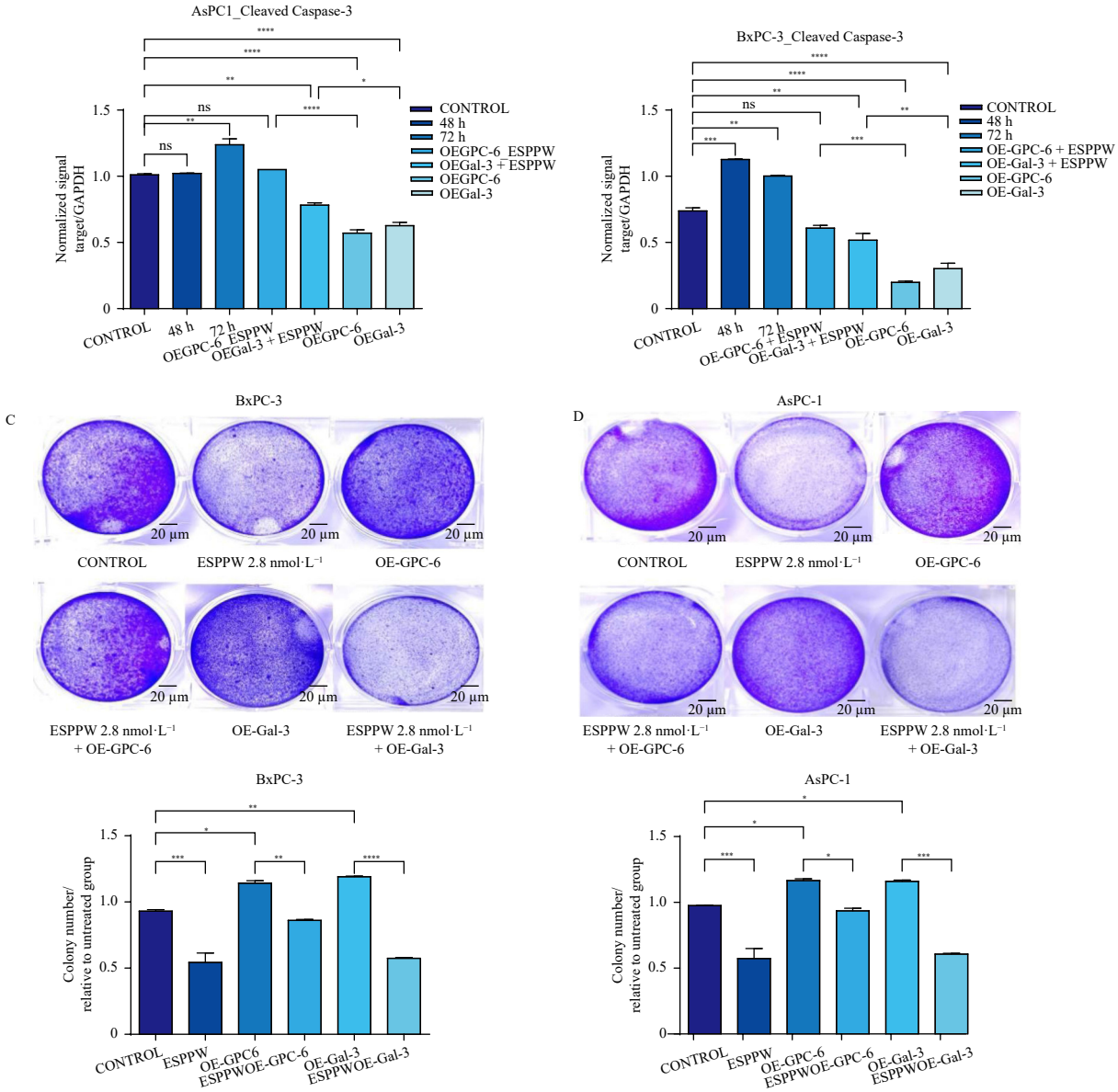

Fig. 8 ESPPW induced cleaved caspase-3 expression and inhibited colony formation in pancreatic cancer cells overexpressing GPC-6 and Gal-3. (A and B) Cleaved caspase-3 expression was evaluated in BxPC-3 and AsPC-1 cells stably overexpressing either GPC-6 or Gal-3 after treatment with ESPPW (2.8 nmol·L^{-1} for 72 h), compared to untreated (vehicle control) cells. (C and D) Representative images of colony formation assays in BxPC-3 and AsPC-1 cells overexpressing GPC-6 and Gal-3 treated with or without 2.8 nmol·L^{-1} ESPPW treatment for 2 weeks. Colonies were stained, imaged, and quantified (scale bar: 20 μm). Data are presented as mean ± SD. All experiments were performed in triplicate. Statistical analysis was conducted using a two-tailed Student's *t*-test. $^{*}P < 0.05$, $^{**}P < 0.01$, $^{***}P < 0.001$, $^{****}P < 0.0001$.

GPC-6 is essential for promoting apoptosis and halting cell cycle progression. Collectively, these results suggest that ESPPW exerts anti-proliferative, anti-tumor, and pro-apoptotic effects through the suppression of Gal-3 and GPC-6. Thus, ESPPW-induced apoptosis in pancreatic cancer cells may be mediated by the downregulation of GPC-6 and Gal-3.

In summary, our findings indicate that the polysaccharide ESPPW derived from *A. platensis* holds promise as a natural anticancer agent. We have characterized ESPPW as primarily composed of glucose and rhamnose. Mechanistically, ESPPW modulates key pathways involved in cell survival and proliferation, including activation of caspase-3 and p53, regulation of cyclin A2, and suppression of oncogenic proteins Gal-3 and GPC-6. To further assess the therapeutic potential of ESPPW, future studies should focus on elucidating its precise mechanism of action through transcriptomic and proteomic profiling and identifying direct molecular targets. Additionally, preclinical safety evaluations and investigations into synergistic effects with established therapies are crucial for advancing ESPPW toward clinical application in pancreatic cancer treatment.

Funding

This work was supported by Shanghai Municipal Science and Technology Major Project, the Strategic Priority Research Program of the Chinese Academy of Sciences (No. XDA12020373), the New Drug Creation and Manufacturing Program (No. 2019ZX09735001), the Ministry of Science and Technology, the People Republic of China and National Natural Science Foundation of China (No. 81903762), and the Key Laboratory for Chemistry and Molecular Engineering of Medicinal Resources (Guangxi Normal University, No. CMEMR2016-B02).

Supporting information

Supporting information for this work can be obtained by contacting the corresponding authors *via* E-mail.

Declaration of competing interest

The authors declare that they have no competing interests.

References

1 Hidalgo M, Cascinu S, Kleeff J, et al. Addressing the challenges of pancreatic cancer: future directions for improving outcomes. *Pancreatology*. 2015;15(1):8-18. https://doi.org/10.1016/j.pan.2014.10.001.

2 Rahib L, Smith BD, Aizenberg R, et al. Projecting cancer incidence and deaths to 2030: the unexpected burden of thyroid, liver, and pancreas cancers in the United States. *Cancer Res*. 2014;74(11):2913-2921. https://doi.org/10.1158/0008-5472.CAN-14-0155.

3 Vincent A, Herman J, Schulick R, et al. Pancreatic cancer. *Lancet*. 2011;378(9791):607-620. https://doi.org/10.1016/S0140-6736(10)62307-0.

4 Neuzillet C, Gaujoux S, Williet N, et al. Pancreatic cancer: French clinical practice guidelines for diagnosis, treatment and follow-up (SNFGE, FFCD, GERCOR, UNICANCER, SFCD, SFED, SFRO, ACHBT, AFC). *Dig Liver Dis*. 2018;50(12):1257-1271. https://doi.org/10.1016/j.dld.2018.08.008.

5 Filmus J, Selleck SB. Glypicans: proteoglycans with a surprise. *J Clin Invest*. 2001;108(4):497-501. https://doi.org/10.1172/JCI200113712.

6 Kirn-Safran C, Farach M, Carson D. Multifunctionality of extracellular and cell surface heparan sulfate proteoglycans. *Cell Mol Life Sci*. 2009;66(21):3421-3434. https://doi.org/10.1007/s00018-009-0096-1.

7 Dinccelik-Aslan M, Gumus-Akay G, Elhan AH, et al. Diagnostic and prognostic significance of glypican 5 and glypican 6 gene expression levels in gastric adenocarcinoma. *Mol Clin Oncol*. 2015;3(3):584-590. https://doi.org/10.3892/mco.2015.486.

8 Gao W, Kim H, Feng M, et al. Inactivation of Wnt signaling by a human antibody that recognizes the heparan sulfate chains of glypican-3 for liver cancer therapy. *Hepatology*. 2014;60(2):576-587. https://doi.org/10.1002/hep.26996.

9 Li N, Spetz MR, Ho M. The role of glypicans in cancer progression and therapy. *J Histochem Cytochem*. 2020;68(12):841-862. https://doi.org/10.1369/0022155420933709.

10 Li J, Kleeff J, Kayed H, et al. Glypican-1 antisense transfection modulates TGF-beta-dependent signaling in Colo-357 pancreatic cancer cells. *Biochem Biophys Res Commun*. 2004;320(4):1148-1155. https://doi.org/10.1016/j.bbrc.2004.06.063.

11 Matsuda K, Maruyama H, Guo F, et al. Glypican-1 is overexpressed in human breast cancer and modulates the mitogenic effects of multiple heparin-binding growth factors in breast cancer cells. *Cancer Res*. 2001;61(14):5562-5569. https://doi.org/10.1016/S0165-4608(01)00481-2.

12 Harada E, Serada S, Fujimoto M, et al. Glypican-1 targeted antibody-based therapy induces preclinical antitumor activity against esophageal squamous cell carcinoma. *Oncotarget*. 2017;8(15):24741-24752. https://doi.org/10.18632/oncotarget.15799.

13 Li N, Fu H, Hewitt SM, et al. Therapeutically targeting glypican-2 *via* single-domain antibody-based chimeric antigen receptors and immunotoxins in neuroblastoma. *Proc Natl Acad Sci U S A*. 2017;114(32):E6623-E6631. https://doi.org/10.1073/pnas.1706055114.

14 Fernandez D, Cercato M, Guereño M, et al. Glypican-3 (GPC3) signaling pathway involved in breast cancer progression. *Cancer Res*. 2018;78(13):4508-4508. https://doi.org/10.1158/1538-7445.AM2018-4508.

15 Sakane H, Yamamoto H, Matsumoto S, et al. Localization of glypican-4 in different membrane microdomains is involved in the regulation of Wnt signaling. *J Cell Sci*. 2012;125(2):449-460. https://doi.org/10.1242/jcs.091876.

16 Li F, Shi W, Capurro M, et al. Glypican-5 stimulates rhabdomyosarcoma cell proliferation by activating Hedgehog signaling. *J Cell Biol*. 2011;192(4):691-704. https://doi.org/10.1083/jcb.201008087.

17 Ni M, Yang X, Liu L, et al. Lentivirus-carrying glypican-6 shRNA inhibits viability and colony formation of human nasopharyngeal carcinoma cells. *Int J Clin Exp Med*. 2018;11(7):6731-6739.

18 Shi W, Kaneiwa T, Cydzik M, et al. Glypican-6 stimulates intestinal elongation by simultaneously regulating Hedgehog and non-canonical Wnt signaling. *Matrix Biol*. 2020;88:19-32. https://doi.org/10.1016/j.matbio.2019.11.002.

19 Yiu GK, Kaunisto A, Chin YR, et al. NFAT promotes carcinoma invasive migration through glypican-6. *Biochem J*. 2011;440(1):157-166. https://doi.org/10.1042/BJ20110530.

20 Dumic J, Dabelic S, Flögel M. Galectin-3: an open-ended story. *Biochim Biophys Acta*. 2006;1760(4):616-635. https://doi.org/10.1016/j.bbagen.2005.12.020.

21 Wehrhan F, Büttner-Herold M, Distel L, et al. Galectin 3 expression in regional lymph nodes and lymph node metastases of oral squamous cell carcinomas. *BMC Cancer*. 2018;18(1):823. https://doi.org/10.1186/s12885-018-4726-6.

22 Kobayashi T, Shimura T, Yajima T, et al. Transient gene silencing of galectin-3 suppresses pancreatic cancer cell migration and invasion through degradation of *β*-catenin. *Int J Cancer*. 2011;129(12):2775-2786. https://doi.org/10.1002/ijc.25946.

23 Yao Y, Zhou L, Liao W, et al. HH1-1, a novel galectin-3 inhibitor, exerts anti-pancreatic cancer activity by blocking galectin-3/EGFR/AKT/FOXO3 signaling pathway. *Carbohydr Polym*. 2019;204:111-123. https://doi.org/10.1016/j.carbpol.2018.10.008.

24 Zhang L, Wang P, Qin Y, et al. RN1, a novel galectin-3 inhibitor, inhibits pancreatic cancer cell growth *in vitro* and *in vivo via* blocking galectin-3 associated signaling pathways. *Oncogene*. 2017;36(9):1297-1308. https://doi.org/10.1038/onc.2016.306.

25 Omstedt PT, von der Decken A, Hedenskog G, et al. Nutritive value of processed *Saccharomyces cerevisiae*, *Scenedesmus obliquus* and *Spirulina platensis* as measured by protein synthesis *in vitro* in rat skeletal muscle. *J Sci Food Agric*. 1973;24(9):1103-1113. https://doi.org/10.1002/jsfa.2740240913.

26 Chang M, Liu K. Arthrospira platensis as future food: a review on functional ingredients, bioactivities and application in the food industry. *Int J Food Sci Technol*. 2024;59(3):1197-1212. https://doi.org/10.1111/ijfs.16882.

27 Piñero EJE, Bermejo BP, Villar del FAM. Antioxidant activity of different fractions of *Spirulina platensis* protean extract. *Farmaco*. 2001;56(5-7):497-500. https://doi.org/10.1016/s0014-827x(01)01084-9.

28 Qu X, Cui S, Xie J, et al. Antitumor studies on the polysacchrides *Spirulina platensis*. *Chin J Mar Drugs*. 2000;19(4):10-14.

29 Koníčková R, Vaňková K, Vaníková J, et al. Anti-cancer effects of blue-green alga *Spirulina platensis*, a natural source of bilirubin-like tetrapyrrolic compounds. *Ann Hepatol*. 2014;13(2):273-283. https://doi.org/10.1016/S1665-2681(19)30891-9.

30 Zhang CQ, Chen X, Ding K. Structural characterization of a galactan from *Dioscorea opposita* Thunb. and its bioactivity on selected Bacteroides strains from human gut microbiota. *Carbohydr Polym*. 2019;218:299-306. https://doi.org/10.1016/j.carbpol.2019.04.084.

31 Honda S, Akao E, Suzuki S, et al. High-performance liquid chromatography of reducing carbohydrates as strongly ultraviolet-absorbing and electrochemically sensitive 1-phenyl-3-methyl-5-pyrazolone derivatives. *Anal Biochem*. 1989;180(2):351-357. https://doi.org/10.1016/0003-2697(89)90444-2.

32 Feng Q, Cao HL, Xu W, et al. Apoptosis induced by genipin in human leukemia K562 cells: involvement of c-Jun *N*-terminal kinase in G_2/M arrest. *Acta Pharmacol Sin*. 2011;32(4):519-527. https://doi.org/10.1038/aps.2010.158.

33 Kobayashi T, Shimura T, Yajima T, et al. Transient silencing of galectin-3 expression promotes both *in vitro* and *in vivo* drug-induced apoptosis of human pancreatic carcinoma cells. *Clin Exp Metastasis*. 2011;28(4):367-376. https://doi.org/10.1007/s10585-011-9376-x.

34 Wu LC, Ho JA, Shieh MC, et al. Antioxidant and antiproliferative activities of Spirulina and Chlorella water extracts. *J Agric Food Chem*. 2005;53(10):4207-4212. https://doi.org/10.1021/jf0479517.

35 Lu Y, Chen Z, Lin Q, et al. Anti-colon cancer effects of *Spirulina* polysaccharide and its mechanism based on 3D models. *Int J Biol Macromol*. 2023;228:559-569. https://doi.org/10.1016/j.ijbiomac.2022.12.244.

36 Chu WL, Lim YW, Radhakrishnan AK, et al. Protective effect of aqueous extract from *Spirulina platensis* against cell death induced by free radicals. *BMC Complement Altern Med*. 2010;10:53. https://doi.org/10.1186/1472-6882-10-53.

37 Marková I, Koníčková R, Vaňková K, et al. Anti-angiogenic effects of the blue-green alga *Arthrospira platensis* on pancreatic cancer. *J Cell Mol Med*. 2020;24(4):2402-2415. https://doi.org/10.1111/jcmm.14922.

38 Moll UM, Wolff S, Speidel D, et al. Transcription-independent pro-apoptotic functions of p53. *Curr Opin Cell Biol*. 2005;17(6):631-636. https://doi.org/10.1016/j.ceb.2005.09.007.

39 Nakahara S, Oka N, Raz A. On the role of galectin-3 in cancer apoptosis. *Apoptosis*. 2005;10(2):267-275. https://doi.org/10.1007/s10495-005-0801-y.

40 Lavra L, Ulivieri A, Rinaldo C, et al. Gal-3 is stimulated by gain-of-function p53 mutations and modulates chemoresistance in anaplastic thyroid carcinomas. *J Pathol*. 2009;218(1):66-75. https://doi.org/10.1002/path.2510.

41 Torii K, Nishizawa K, Kawasaki A, et al. Anti-apoptotic action of Wnt5a in dermal fibroblasts is mediated by the PKA signaling pathways. *Cell Signal*. 2008;20(7):1256-1266. https://doi.org/10.1016/j.cellsig.2008.02.013.

42 Tang Q, Chen C, Zhang Y, et al. Wnt5a regulates the cell proliferation and adipogenesis *via* MAPK-independent pathway in early stage of obesity. *Cell Biol Int*. 2018;42(1):63-74. https://doi.org/10.1002/cbin.10862.

43 Osone S, Hosoi H, Kuwahara Y, et al. Fenretinide induces sustained-activation of JNK/p38 MAPK and apoptosis in a reactive oxygen species-dependent manner in neuroblastoma cells. *Int J Cancer*. 2004;112(2):219-224. https://doi.org/10.1002/ijc.20412.

44 Zhou Y, Kipps TJ, Zhang S. Wnt5a signaling in normal and cancer stem cells. *Stem Cells Int*. 2017;2017(1):5295286. https://doi.org/10.1155/2017/5295286.

45 Melleby AO, Strand ME, Romaine A, et al. The heparan sulfate proteoglycan glypican-6 is upregulated in the failing heart, and regulates cardiomyocyte growth through ERK1/2 signaling. *PLoS One*. 2016;11(10):e0165079. https://doi.org/10.1371/journal.pone.0165079.

46 Fukushi J, Makagiansar IT, Stallcup WB. NG2 proteoglycan promotes endothelial cell motility and angiogenesis *via* engagement of galectin-3 and α3β1 integrin. *Mol Biol Cell*. 2004;15(8):3580-3590. https://doi.org/10.1091/mbc.e04-03-0236.

47 Wen Y, Makagiansar IT, Fukushi J, et al. Molecular basis of interaction between NG2 proteoglycan and galectin-3. *J Cell Biochem*. 2006;98(1):115-127. https://doi.org/10.1002/jcb.20768.